PREPRINT

A "reduced" distributed monopole model for the efficient prediction of energy transfer in condensed phases

Corrado Bacchiocchi[a], Emmanuelle Hennebicq[b], Silvia Orlandi[a], Luca Muccioli[a], David Beljonne[c], and Claudio Zannoni*,[a]

[a] *Dipartimento di Chimica Fisica e Inorganica and INSTM, Università, Viale Risorgimento 4, I-40136 Bologna, Italy*

[b] *Laboratory for Chemistry of Novel Materials and Center for Research in Molecular Electronics and Photonics, University of Mons-Hainaut, Place du Parc 20, B-7000 Mons, Belgium*

[c] *Laboratory for Chemistry of Novel Materials and Center for Research in Molecular Electronics and Photonics, University of Mons-Hainaut, Place du Parc 20, B-7000 Mons, Belgium and School of Chemistry and Biochemistry and Center for Organic Photonics and Electronics, Georgia Institute of Technology, Atlanta, Georgia 30332-0400*

* Corresponding Author: Phone/Fax: + 39 051 644 7012.
E-mail: Claudio.Zannoni@unibo.it.
URL: http://www.fci.unibo.it/~bebo/z/.

Abstract

We propose a methodology for the realistic simulation and prediction of resonance energy transfer in condensed phases based on a combination of computer simulations of phase morphologies and of a distributed monopole model for the radiationless transfer. The heavy computational demands of the method are moderated by the introduction of a transition charges reduction scheme, originally developed for ground state interactions [Berardi, R. *et al. Chem. Phys. Lett.* **2004**, *389*, 373]. We demonstrate the scheme for a condensed glass phase formed by perylene monoimide end-capped 9,9-(di *n,n*)octylfluorene trimers, recently studied as light-harvesting materials, where we couple a coarse-grained Monte Carlo simulation of the molecular organization and a master equation approach modeling the energy diffusion process.

Keywords: *photovoltaics, Monte Carlo, computer simulations, excited-state, oligofluorenes, solar cells*

1 Introduction

The "hopping" of the electronic energy from one excited chromophore (donor) to another (acceptor), termed "resonance energy transfer" (RET), is an ubiquitous mechanism involved in many fundamental biochemical processes such as photosynthesis [1,2]. During the last ten to fifteen years there has been a flourishing of activity in the field of organic electronics, particularly trying to achieve and take advantage of fast and directional energy migration, e.g. to obtain efficient color conversion in light-emitting displays [3–5] or to improve harvesting of the electronic excitations at dissociation zones in solar cells [6–9].

In particular, the computational study of Förster-type energy transfer [10–12], based on the so-called "weak coupling limit" of the radiationless transition theory (i.e. assuming that the RET process occurs after vibrational relaxation has taken place in the donor excited state), is generally accomplished by approximating the electronic coupling between donor and acceptor on the basis of the interaction between point transition dipole moments. This approach, however, is strictly valid only when the size of the chromophores is small compared to the intermolecular separations and has been widely used to describe RET among chromophores in systems where distances are of the order of several nanometers, e.g. in a relatively diluted matrix. In a condensed phase formed by oligomeric or polymeric molecules, the average distance among neighboring chromophores is comparable or even much smaller than the molecular dimensions. Therefore it is more appropriate to use, rather than a single transition dipole, a distributed monopole model [13–15] which takes into account the three dimensional shape of the donor and acceptor, since the total electronic coupling is estimated as the sum over atomic transition charge densities [16,17].

As RET depends anyway on the positions and orientations of the molecules involved, a key part of any such calculation relies on the knowledge of the morphology of the condensed phase and more specifically of a sufficient number of representative molecular configurations of the system, such as those that can be generated by a computer simulation via Monte Carlo (MC) or Molecular Dynamics (MD) techniques.

In this study we generalize a combined MC simulations and master equation approach [18,19] to study the evolution of the RET process in a condensed phase formed by complex molecules with the possibility of intra and intermolecular RET. The time dependence of the RET process is modeled in a step-by-step fashion by solving the master equation of the excitation probability for small time intervals. This approach can be further generalized to model RET diffusion in low viscosity fluid phases, e.g. by coupling the calculation of the energy hopping process with MD simulations [20]. Implementing the distributed monopoles approach [13–15] requires a heavy use of computational resources due to sheer number of transition charge contributions to be summed over. Here a charge number reduction technique [21] (see below) has been adopted in the simulations to speed-up the calculation of the interchromophore RET rate which represents a significant portion of the CPU time. Such a strategy is fundamental in view of the realistic prediction of the overall efficiency and direction of the transfer in a real device, which represents our long-term goal.

As a model system to test the reduced scheme for the calculation of the electronic couplings, we have considered a condensed phase formed by 9,9-(di *n,n*)octylfluorene trimers (hereafter: terfluorene) α, ω covalently linked with two *N*-(2,6-dimethylphenyl)-3,4-dicarbonicacidimide-perylenes (hereafter simply: perylene; the structure of the compound is shown in Figure 1). The choice was motivated by the possibility of studying both intra and intermolecular excitation transfer processes in the bulk and by the body of experimental data that are available for this molecule or for systems of close chemical similarity [22–24].

2 Simulation of glass phase morphologies

Linear dioctyl polyfluorene polymer chains are known to form crystalline and liquid-crystalline phases both in bulk and thin film samples [25,26], showing a remarkably high intermolecular order. On the other hand fluorene dimers and trimers hardly form liquid-crystalline phases [27], if not suitably substituted with linear alkyl chains at their ends [28,29], and exhibit only a glassy solid phase below the isotropic one. The end-capping of such polymers and oligomers with bulky groups like perylenes is expected to further suppress their self-assembling abilities, consistently with the experimental observation of room temperature amorphous solids which decompose above 400 K [22]. In such systems the RET process from the fluorene chain to the end-capping groups is very efficient, while it is slower and competes with radiative decay in solution [22], probably because limited by the slow intramolecular exciton diffusion along the backbone, as it has been demonstrated for polyindenofluorenes [17]. It is therefore a reasonable choice for this study to investigate the process occurring in the glass phase, whose coarse-grained morphology has been derived here through MC simulations of a multisite Gay-Berne (GB) molecular model [30,31] described below.

2.1 Gay-Berne molecular model

We opted for modeling each chromophore (i.e. two identical perylenes and the terfluorene) with the heterogeneous biaxial GB potential [32], which easily allows for the simulation of multicomponent systems constituted by thousands of molecules, described as attractive–repulsive ellipsoids. In this particular case, the molecule is treated as formed by five fragments: one central terfluorene, two

end-capping perylenes and two dimethylbenzenes. Fragments are modeled as five ellipsoids rigidly attached and partially overlapping (see Figure 1). Once arbitrarily set the potential orientational-tuning exponents μ and ν to the value of 1 and 0 respectively (see [32] for the explicit equations), the shape and the homogeneous and heterogeneous interactions are completely defined by each ellipsoid axis lengths σ_x, σ_y, σ_z and interaction energies ϵ_x, ϵ_y, ϵ_z. To derive these parameters, both intermolecular energy and contact distances of each couple of identical fragments, at their equilibrium Austin model 1 (AM1) [33] geometry, have been evaluated along the inertial axis directions at molecular mechanics level, using the AMBER Force Field [34] and ground state AM1 charges. Contact distances and ellipsoid centers were subsequently adjusted in order to completely include their atomistic counterparts (see Figure 1) and avoid unrealistically short charge–charge distances in the computation of RET. An exception has been done in the evaluation of the contact distance between two parallel terfluorene units, which has been directly taken from the distance between aligned polyfluorene chains (12.8–13.0 Å) measured by X-ray diffraction in the liquid-crystalline phase [25, 26]. Considering the finding of Jäckel *et al.* [35] that similarly end-capped terfluorenes should present predominantly a bent shape in thin films, and that AM1 calculations of such systems gave an angle between the two perylene z axes of about 120°, we have adopted this geometry in the simulation. The final GB parameters, site positions and orientations are reported in Table 1.

2.2 Monte Carlo simulation

Molecular organizations have been produced via MC simulations at constant number of molecules, N, pressure, P and temperature, T, using periodic boundary conditions and the minimum image convention [36]. The molecular system was formed by $N = 10^3$ particles at adimensional pressure $P^* = 5$. Exploratory runs showed that the system undergoes a liquid–solid phase transition at a dimensionless temperature T^* of about 5.5. To reproduce the formation of a glass, we first equilibrated for 200 kcycles (1 kcycle = N attempted MC moves) a low density sample (at $T^* = 20$), subsequently used as a starting point for a long production run of 1 million cycles. During this run, 10^2 statistically independent configurations were saved, one each 10 kcycles. These stored configurations were separately driven to the glass state by cooling them down at the temperature $T^* = 2$ with 30 kcycles-long MC simulations. The 10^2 final configurations were used as an input for the RET simulation (see below). A typical snapshot of such a configuration, showing the dense packing between the oligomers, is shown in Figure 2, where we have assigned a color to each molecule according to its orientation, and we can notice the presence of locally ordered domains in an essentially isotropic matrix.

3 Modeling and simulation of energy transfer

A usual approach to calculate the electronic coupling that promotes radiationless RET is to assume, as in Förster theory, a point dipole model. This model is strictly valid only when the separation between charges is small with respect to the intermolecular separations. Here we adopt a different and more general model which takes into account the three dimensional shape of the interacting molecules [13].

3.1 Distributed and reduced Monopole Model for the energy transfer rates

In a condensed phase, e.g. that of an amorphous solid formed by oligomeric or polymeric molecules of interest here, a more appropriate approach to calculate the total electronic coupling, V_{DA}, is to use a distributed monopole model [13–15], where V_{DA} is estimated as the sum over the atomic transition charge densities (in the following "transition charges" or, simply, "charges" will be also used) and can therefore take into account the spatial shape of the donor and acceptor moieties:

$$V_{DA} = \frac{1}{4\pi\epsilon_0} \sum_m \sum_n \frac{q_D(m)\; q_A(n)}{\mathbf{r}_{mn}} \,, \tag{1}$$

where the summations run over all atoms m and n on the donor D and acceptor A. $\mathbf{r}_{mn}$ is the distance between m and n, and $q_D(m)$, $q_A(n)$ are transition charges on atoms m, n for the lowest optical $g \rightarrow e$ excitation of donor and acceptor, calculated at the excited and ground state equilibrium geometries for donor and acceptor respectively, using the intermediate neglect of differential overlap, single configuration interaction method (INDO-SCI) [37].

Within the weak coupling regime and under the assumption of independent vibrational modes (displaced quadratic potential energy surfaces are considered for ground and excited electronic state) coupled to the donor and the acceptor transitions involved in the energy transfer process, the following expression for the transfer rate is obtained [38]:

$$k_{DA} = \frac{2\pi}{\hbar}\, V_{DA}^2 \int_{-\infty}^{+\infty} dE\; \sigma_D(E)\, \sigma_A(E) \,, \tag{2}$$

where the integral represents the spectral overlap, J_{DA}, that was estimated on the basis of the simulated donor emission, $\sigma_D(E)$ and acceptor absorption $\sigma_A(E)$ spectra, normalized on an energy scale, of oligoindenofluorenes and perylene reported in Ref. [17] where a two-mode displaced harmonic oscillator model has been considered. We made here the assumption that optical properties of terfluorenes can simply be related to the optical spectra of dimers of indenofluorene. The systems are very similar and their electronic excited states are expected to couple to similar vibrational

modes. Within this very simple model, the spectral overlaps between terfluorene (TER) and perylene (PER), acting either as a donor or acceptor, result to be: $J_{DA} = 0.94$ eV^{-1} (TER→PER), 0.81 eV^{-1} (PER→PER), 0.11 eV^{-1} (TER→TER) and 0.00 eV^{-1} (PER→TER).

Due to the large number of transition charges and to the long range nature of the interaction the use of equation 1 in the calculation of the RET on a system composed by thousands of molecules (*e. g.* in a real device simulation), is quite expensive in terms of computation time, analogously to what happens when calculating Coulomb interactions. To overcome this technical problem, we introduce here a charge number reduction method ("reduced monopoles"), originally developed to speed-up calculations of electrostatic interactions [21] with a minimal loss of accuracy.

The underlying idea of the reduction scheme is that, outside the molecular surface, the electrostatic like field corresponding to a certain distribution of atomic transition charges, can be in general well reproduced by a lower number of charges, not necessarily positioned at the atomic centers but simply lying inside the van der Waals volume of the molecule. This is accomplished through a genetic algorithm which evolves a population of sets of charges, optimizing the fit through a minimization of the mean square difference between the atomistic and the reduced potential on a grid of points surrounding the molecular volume [21]. The approach can be applied identically both to ground state charges and transition charges, as we do here, with the notable difference that, as the electronic coupling, V_{DA}, appears squared in equation 2, for achieving the same level of quality on the final result, a higher accuracy in the optimal set of charges is required when modeling RET. Differently from reference [21] where concentric shells and linear least square minimization were used, in this study we have employed a rectangular mesh of test points in the evaluation of the single sets of charges, whose values were derived by a non-linear fit of the potential on the grid points with the classic Nelder-Mead algorithm.

3.2 Atomic transition charge densities

The ground and excited state geometries of a model of the terfluorene molecule and of the perylene derivative were optimized separately at the AM1 configuration interaction level [33,39], starting from fully planar conformations for each. Like in [17], the alkyl chains of the conjugated oligomer were replaced by methyl groups for reducing the computational burden and therefore were implicitly considered only in the morphology derivation and not in the electronic coupling calculation. As described in [16], a subset of electronic configurations is selected using perturbation theory from the list generated by a full configuration interaction over a defined window of molecular orbitals (active space) which is increased until convergence of the results. The optimized geometries were then used as input for excited state calculations performed by means of the INDO-SCI formalism. As an output of these calculations, we obtain the excitation energies and transition dipole matrix elements, as well as the corresponding atomic transition charges [40] associated with the $g \rightarrow e$ and $e \rightarrow g$ transitions.

To simplify our treatment, both intra- and intermolecular transfer rates, have been calculated by adopting the same approach described in the previous section. In doing so, we assume that the excitation is localized on a single perylene or terfluorene moiety which are essentially decoupled, due to their different chemical nature and the ≈60° torsion angle (at the AM1 level) between their conjugate systems. We must consider, however, that this approximation is not strictly valid, as both experiment and theory [23,24] suggest that the lowest excited state, in related chemical structures, slightly expands from the perylene end-cap onto the neighbor phenylene-based conjugated segment. Thus, the intramolecular RET process might also be mediated by through-bond interactions. Though disentangling between through-space and through-bond contributions to the overall intramolecular rate is not the main issue of this work, we have repeated our simulations for different values of the terfluorene-to-perylene RET rate to test the robustness of our approach with respect to the possible scenarios (fast or slow intramolecular excitation transfer). Conversely, in oligofluorenes the excitation has been found to be delocalized on at least two consecutive monomeric units [41]; as a consequence the whole terfluorene fragment can be treated as a unique chromophoric entity.

3.3 Modeling the energy transfer process

In the weak coupling regime, each chromophore, depending upon its excitation level, can act either as a donor or an acceptor of electronic energy. According to the theory, the overall RET process is composed by individual transfers ("hops") from one excited chromophore to another where each "hop" is uncorrelated with the previous. This RET can be therefore modeled by a stochastic process with N_c states corresponding to the excitation energy being on one of the N_c chromophores involved [18,42]. The evolution of the RET process is described in terms of the probability, $P_{ET_i}(t)$, of finding the excitation on the i-th molecule at time t and the rate of the transfer, Π_{ij} ($\equiv k_{DA}$ for $i \neq j$), of this excitation between a donor i and an acceptor j. The following master equation holds [18,19]:

$$\dot{\mathbf{P}}_{ET}(t) = \mathbf{\Pi}(t)\,\mathbf{P}_{ET}(t), \tag{3}$$

where the vector

$$\mathbf{P}_{ET}(t) = P_{ET_1}(\mathbf{r}_1, \mathbf{\Omega}_1), P_{ET_2}(\mathbf{r}_2, \mathbf{\Omega}_2), \ldots, P_{ET_{N_c}}(\mathbf{r}_{N_c}, \mathbf{\Omega}_{N_c}) \tag{4}$$

contains the probabilities that each chromophore i, with position $\mathbf{r}_i$ and orientation $\mathbf{\Omega}_i$, where $\mathbf{\Omega} \equiv (\alpha, \beta, \gamma)$ is the orientation in terms of Euler angles [43], is excited at time t. In the assumption of fixed molecular orientations and positions, the kinetic matrix, $\mathbf{\Pi}$, becomes time independent [18,19]. In this case the evolution is a simple Markov process and equation 3 has the formal solution:

$$\mathbf{P}_{ET}(t) = e^{t\mathbf{\Pi}}\,\mathbf{P}_{ET}(0)\,, \tag{5}$$

which can be handled via numerical diagonalization of the real matrix $\mathbf{\Pi}$:

$$\mathbf{P}_{ET}(t) = \mathbf{X}\,e^{\mathbf{\Lambda}t}\,\mathbf{X}^{-1}\mathbf{P}_{ET}(0)\;, \tag{6}$$

where $\mathbf{X}$ is the matrix of eigenvectors of $\mathbf{\Pi}$, $\mathbf{\Lambda}$ is the vector of eigenvalues and $\mathbf{P}_{ET}(0)$ is the initial condition. Unfortunately this "exact" solution of the master equation is still quite time consuming, the computation of all eigenvalues and eigenvectors of a $N_c \times N_c$ (with $N_c = 3 \times 10^3$) nonsymmetric matrix, required in the simulation of a system of 10^3 molecules, takes about 2.5 h on a single Xeon processor (1.7 GHz), using optimized LAPACK [44] fortran routines. A more convenient approach is therefore to use the second order approximation [20]

$$\mathbf{P}_{ET}(t+\delta t) \;\approx \mathbf{W}\,\mathbf{P}_{ET}(t)\;, \tag{7}$$

where

$$\mathbf{W} = \mathbf{I} + \delta t\,\mathbf{\Pi} + \frac{1}{2}\,(\delta t)^2\,\mathbf{\Pi}^2\,, \tag{8}$$

$\mathbf{I}$ is the identity matrix and δt is a time interval small enough, conveniently chosen. The excitation probability after n time steps is given by the product:

$$\mathbf{P}_{ET}(t+n\delta t) \approx \mathbf{W}^n\,\mathbf{P}_{ET}(t)\,. \tag{9}$$

This step-by-step algorithm is analogous to that described in a previous work [20]. In the present model, due to the high viscosity of the system, we can assume that, within the fast RET time scale, the molecular orientations and positions are fixed; therefore the kinetic matrix $\mathbf{\Pi}$, and the evolution operator $\mathbf{W}$, are time independent. To ensure stability of the algorithm, δt must be about two orders of magnitude smaller than the time scale of the fastest process occurring in the system, which, in our case, is given by the lifetime of the excitation on the initially excited terfluorene. Smaller values will provide better approximations but will also require a larger number of time steps and a larger computation time. With $\delta t = 1$ fs, the value typically used in our simulations, the difference between the RET evolution calculated with the step-by-step algorithm and that obtained via numerical diagonalization [18] was smaller than 1 %. We neglect the radiative decay of the chromophores since this process would occur on a much longer time scale (ns, instead of ps for the RET process) and therefore it would not significantly affect the results. According to the conditions adopted in a single photon counting fluorescence experiment, we assume that only one terfluorene chromophore is excited at time zero. In a preliminary series of simulations, the calculation of the RET process was repeated over 10^2 different MC equilibrium configurations; for each one, the initially excited terfluorene was chosen at random, using a congruential pseudo-random number generator fortran routine, tested for randomness; the results were averaged. In the final simulations, to further improve the statistic, for each MC configuration the calculation was repeated 10 times, each time using as a starting condition a different excited terfluorene.

4 Results and Discussions

We show first of all the results obtained for the RET using the procedure described above with the full set of transition charges, that constitutes our reference set of results. Then we shall validate the charge reduction procedure, showing the effects of decreasing the set of charges. Finally, we present an application of the method for investigating the effects of changing the intramolecular to intermolecular transfer rates.

In a recent work, some of us [17] compared the intra vs. inter RET rate in a condensed phase formed by oligo and polyindenofluorenes end-capped with a perylene derivative finding the intra-chain transfer rates from oligoindenofluorenes of various sizes to the end-capping perylenes consistently lower than the corresponding interchain transfer rates which were calculated assuming the two chromophores closely packed in a cofacial arrangement at a distance (determined at molecular mechanics level) of 4.2 Å. In the present model, we calculated a terfluorene-to-perylene intramolecular transfer rate of 79 ps^{-1} whereas a typical intermolecular rate for a nearest-neighbor distance of 13 Å (corresponding to the maximum of the terfluorene–perylene radial correlation function), is in the range 1–10 ps^{-1}, depending also on interchromophore orientation.

In this work we address also the effect of transfer rate and translational-orientational disorder of the time dependence of the excitation probability. Figure 3 shows the time evolution of RET modeled with the full set of transition charges. We notice that the initially excited terfluorene features a very rapid exponential decay of the excitation probability (Figure 3, curve (a); the final portion of the decay is expanded in the inset). The ultrafast time scale of this decay (≈10 fs) is mainly due to the relatively high intramolecular transfer rate between linked terfluorene and perylene (both chromophores posses strong transition dipoles of about 10 D) and is enhanced by the fact that two acceptors are attached to each donor.

Following this transfer, the excitation probability of the two perylenes attached to the first excited terfluorene quickly reaches a maximum and is followed by a slower decay (Figure 3, curve (b)), providing a time scale for the transition from the intramolecular to the intermolecular RET regime (before and after the maximum, respectively). Correspondingly, the time dependence of the excitation probability of all the other perylene chromophores combined, i.e. excluding the two perylenes belonging to the initially excited molecule, shows an asymptotic increase (Figure 3, curve (c)) which indicates that, at longer times, the excitation can be found only on perylenes.

At longer times and in the absence of other deactivation mechanisms on the ps time scale, the excitation probability will tend to be the same on each perylene, with an asymptotic value of $1/N_p$, were N_p is the total number of perylenes. Since curve (c) in Figure 3 represents the whole perylene population, with the exception of the two perylenes belonging to the initially excited molecule, the asymptotic value of this curve will be $1 - 2/N_p$.

Finally, curve (d), in the inset of Figure 3, represents the excitation probability of all the terfluorene chromophores combined, with the exception of the initially excited one. The curve exhibits an extremely small peak at very short times indicating that the overall rate of the energy that is transferred *to* the terfluorene population is quickly surpassed by the rate of the energy transferred *from* the terfluorenes to the perylenes. In fact, only the initially excited terfluorene can transfer to the other terfluorenes and the efficiency of this transfer, in keeping with the different spectral overlaps, J_{DA}, presented above, appears to be much lower than the transfer from these terfluorenes to either their end-cap perylenes or the perylenes on other molecules. In particular, we observe that this peak occurs at a time slightly shorter than the maximum of curve (b), indicating that the excitation of the entire terfluorene population starts to decrease even before the excitation on the first two perylenes has reached the maximum.

Proceeding to the charge reduction method validation, three charge reduction schemes (CRS) have been preliminarily tested (see Table 2) in a series of RET simulations and compared to simulations done with the complete set of transition charges (full charges). In each CRS the two full sets of charges, associated with the $g \rightarrow e$ and $e \rightarrow g$ transitions on each chromophore, where reduced to the same number of charges. Namely, the original 52 charges on perylene were reduced to 11 whereas the 83 charges on terfluorene were reduced to 6 in CRS1, 4 in CRS2 and 2 in CRS3. In Figure 4 we see, as an example, the transition charge distribution, associated with the $g \rightarrow e$ transition, for perylene (a) and terfluorene (b), obtained from the full set of charges, and from a reduction scheme involving 11 charges on perylene (c) and 6 charges on terfluorene (d), together with their position in the molecular frame (e), (f). The color-coding shows the good reproduction of the transition charge map. As a more severe test of the approximation scheme, Figure 5 shows maps of the RET rate (ps^{-1}), calculated with full charges (a) or with CRS1, CRS2 and CRS3 (b, c and d, respectively), from a terfluorene (donor), fixed at the origin, to a perylene (acceptor) placed at the sites of a grid from -20 to 20 Å at 1 Å resolution, on the xy plane. Molecular main axes are along z and the planar cores of the two chromophores are parallel. Interchromophore separations corresponding to an interaction energy larger than $3kT$ ($T = 298.2K$), estimated using simply the Lennard-Jones parameters of the AMBER force field [34], where removed from the grid. The map in (a) is color-coded according to the value of the donor–acceptor RET rate (ps^{-1}) whereas the other maps are color-coded according to the percent deviation from (a) of the three CRS. At an interchromophore distance of approximately 13 Å, corresponding to the maximum of the terfluorene–perylene radial correlation function (i.e. the average nearest-neighbor distance), the positive (red) and negative (blue) deviations are quite encouraging, being approximately within $\pm 2\%$ for *CRS1* and *CRS2* and increase to $\pm 5\%$ for CRS3.

As a more realistic test, in Figure 6 the time dependence of the excitation probability calculated using the full set of transition charges (see Figure 3) is compared with that calculated by adopting the three CRS. Although the agreement is generally good, we see that, at very short times, all the three CRS show an appreciable deviation, larger than the statistical uncertainties, from the full charge calculation (see inset I of Figure 6). At slightly longer times, in the intermolecular regime, this deviation can be found, instead, to be negligible, being within the uncertainties of the calculation (inset II).

To improve the CRS at shorter times (and hence at shorter distances), we adopted a scheme where two different charge reductions are employed, according to the level of detail required to describe interactions at different distances. In practice, we chose to modify *CRS3* (*11* charges on perylene and 2 on terfluorene), which showed the larger deviation at shorter times, by using the full set of transition charges to model the intramolecular RET, while still adopting the charge reduction for all other transfers. In Figure 7 this "improved" version of the CRS3, labeled ICRS3 (see Table 2), is compared to the full calculation. We clearly see that the ICRS3 scheme reproduces very well the full charge RET evolution even at shorter times and always within the statistical uncertainties.

In summary, despite the quite relevant reduction in the number of charges (11 vs. 52 on perylene and 6, 4 or 2 vs. 83 on terfluorene) adopted in the calculation, the configuration-averaged evolution of the intermolecular RET is satisfactorily reproduced in all cases, whereas relatively larger deviations are observed at shorter times, i.e. in the intramolecular regime. This result can be rationalized by considering the spectroscopic nature of the chromophores involved. In fact, the spectral

overlap, J_{DA}, of the terfluorene-to-perylene and of the perylene-to-perylene RET is larger than that of terfluorene-to-terfluorene whereas the perylene-to-terfluorene spectral overlap is negligible. The initially excited terfluorene can be regarded as a sort of sensitizer for the perylene population since the process, after the initial and essentially intramolecular transfer, is dominated by the diffusion of the excitation among perylene chromophores. In this situation, it appears reasonable that even a drastic charge reduction in the description of the terfluorene charge distribution (2 charges vs. 83) has only a small effect on the overall simulation of the RET.

A more strict test for our charge reduction method should therefore involve a further reduction of charges on the perylene chromophore as well. A fourth scheme, labeled ICRS4 (see Table 2), was tested. The intermolecular transfer rates were calculated using only 4 charges vs. 52 on perylene and, as in ICRS3, 2 charges vs. 83 on terfluorene. The full set of transition charges was used to model the intramolecular RET. Results for this new scheme are shown in Figure 7. The scheme exhibits a slightly larger deviation from the full charge calculation compared to ICRS3 but, also in this case, within the statistical uncertainty.

In both ICRS3 and ICRS4 the intramolecular transfer rates are calculated using the full set of transition charges whereas the reduced set is used for all the other transfers. This approach significantly improved the RET simulation at shorter times, providing results nearly identical to those obtained in the full charge calculation. The extra cost, in terms of computing time, of this method with respect to the adoption of the same charge reduction for all transfer rates, is negligible since the number of interactions to be treated in full detail is small, being proportional to the number of chromophores, N_c, in the system, compared to the total number of interactions which is proportional to N_c^2. Last column of Table 2 lists the computation speed factors (proportional to the decrease of the computing time with respect to the full charge calculation) for the different CRS adopted in the simulations.

The relatively fast computing times make it possible to investigate the consequences of different scenarios on the RET. For instance, here the scheme ICRS3 was adopted in a further simulation of RET where the intramolecular transfer was artificially slowed down in order to explore the case, opposite to the one previously considered, of a diffusion process limited by the intramolecular transfer rate from the terfluorene to the perylene moiety. In this way we also address the issue of a possible through-bond contribution to the intramolecular RET which may give rise to rates at variance with the ones foreseen by the weak coupling limit model. The resulting RET evolution, where the intramolecular hopping rate was arbitrarily decreased by a factor of 10, is shown in Figure 8 ("INTRA < INTER", dashed lines), compared to the previous case ("INTRA > INTER", solid lines). The slowing down of the intramolecular RET determines a marked decrease of the excitation probability maximum of the two perylenes attached to the first excited terfluorene and a shift to longer times, in keeping with the slower decay of the initially excited terfluorene. The overall evolution of the RET among the other molecules is, instead, only slightly affected, since it is still dominated by the intermolecular transfer rate among the perylene chromophores which is about eight times larger than the transfer rate among the terfluorenes. From an experimental point of view, even in the case "INTRA < INTER", the emission of the initially excited terfluorene would be completely quenched by the transfer to the end-capping perylenes. This result is in qualitative agreement with that obtained by Ego *et al.* [22] for systems of close chemical similarity formed by perylene end-capped oligo and polyfluorenes, where the observed emission comes solely from the perylene units.

5 Conclusions

We have proposed a method for the realistic simulation of resonance energy transfer (RET) in condensed phases. The method generalizes our previous approaches [18,20] combining coarse grained computer simulations, to obtain representative sets of molecular organizations, and a Markov process, modeling RET between chromophores. The transfer is calculated using an improved Förster approach based on distributed transitions monopoles [13]. This approach effectively allows modeling of RET between different parts of the same molecule (intramolecular transfer) as well as of different molecules (intermolecular transfer) in condensed phases. This is important for the complex oligomers, as the perylene-monoimide-N-dimethylbenzene end-capped 9,9-(di n,n)octylfluorene trimers treated here and in all cases where molecules of dimensions larger than their typical intermolecular distances are employed. The introduction of a transition charge on every atom brings the inevitable penalty of a high computational cost, similar to that of extensive electrostatic summations in the simulation of complex polar molecules. To drastically reduce this computational load, we have introduced and validated a charge reduction scheme (CRS), that allows an excellent approximation to the transfer employing a reduced number of suitably positioned effective transition charges. We show that the CRS is particularly effective for the intermolecular contributions, while the full set of charges can be used, at a limited computational cost, for the intramolecular RET.

Given this possibility of realistic simulation of intra and intermolecular RET in condensed phases and of investigating the effect of changes in morphology, we believe the present method to be a powerful and potentially very useful tool for the simulation of the RET process in a variety of problems relevant to organic electronics.

Acknowledgments

We thank EU IP project NAIMO ("Nanoscale integrated processing of self-organizing multifunctional organic materials", NMP-CT-2004-500355) and EU STREP project MODECOM ("Modelling electroactive conjugated materials at the multiscale", NMP-CT-2006-016434). EH and DB are postdoctoral researcher and senior research associate of the Belgian National Science Foundation (FNRS), respectively.

References and Notes

(1) Sundström, V.; Pullerits, T.; Grondelle, R. V. *J. Phys. Chem. B* **1999**, *103*, 2327.

(2) Scholes, G. D.; Fleming, G. R. *J. Phys. Chem. B* **2000**, *104*, 1854.

(3) Lee, J.-I.; Kang, I.-N.; Hwang, D.-H.; Shim, H.-K.; Jeoung, S. C.; Kim, D. *Chem. Mater.* **1996**, *8*, 1925.

(4) List, E. W. J.; Holzer, L.; Tasch, S.; Leising, G.; Scherf, U.; Müllen, K.; Catellani, M.; Luzzati, S. *Solid-State Commun.* **1999**, *109*, 455.

(5) Wang, H.-L.; McBranch, D.; Klimov, V. I.; Helgerson, R.; Wudl, F. *Chem. Phys. Lett.* **1999**, *315*, 173.

(6) Sariciftci, N. S.; Smilowitz, L.; Heeger, A. J. Wudl, F. *Science* **1992**, *258*, 1474.

(7) Halls, J. J.; Walsh, C. A.; Greenham, N.; Marseglia, E. A.; Friend, R. H.; Moratti, S. C.; Holmes, A. B. *Nature* **1995**, *376*, 498.

(8) Yu, G.; Gao, J.; Hummelen, J. C.; Wudl, F.; Heeger, A. J. *Science* **1995**, *270*, 1789.

(9) Watkins, P. K.; Walker, A. B.; Verschoor, G L. B. *Nano Lett.* **2005**, *5*, 4697.

(10) Förster, T. *Ann. Phys. (Leipzig)* **1948**, *2*, 55.

(11) Förster, T. In *Modern Quantum Chemistry*; Sinanoğlu, O., Ed.; Academic Press, 1965; page 93.

(12) Jang, S.; Newton, M. D.; Silbey, R. J. *Phys. Rev. Lett.* **2004**, *92*, 218301.

(13) Marguet, S.; Markovitsi, D.; Millié, P.; Sigal, H.; Kumar, S. *J. Phys. Chem. B* **1998**, *102*, 4697.

(14) Krueger, B. P.; Scholes, G. D.; Fleming, G. R. *J. Phys. Chem. B* **1998**, *102*, 5378.

(15) Beljonne, D.; Cornil, J.; Silbey, R.; Millié, P.; Brédas, J. L. *J. Chem. Phys.* **2000**, *112*, 4749.

(16) Beljonne, D.; Pourtois, G.; Silva, C.; Hennebicq, E.; Herz, L. M.; Friend, R. H.; Scholes, G. D.; Setayesh, S.; Müllen, K.; Brédas, J. L. *Proc. Natl. Acad. Sci. USA* **2002**, *99*, 10982.

(17) Hennebicq, E.; Pourtois, G.; Scholes, G. D.; Herz, L. M.; Russell, D. M.; Silva, C.; Setayesh, S.; Grimsdale, A. C.; Müllen, K.; Brédas, J. L.; Beljonne, D. *J. Am. Chem. Soc.* **2005**, *127*, 4744.

(18) Bacchiocchi, C.; Zannoni, C. *Chem. Phys. Lett.* **1997**, *268*, 541.

(19) Bacchiocchi, C.; Zannoni, C. *Phys. Rev. E* **1998**, *58*, 3237.

(20) Bacchiocchi, C.; Brunelli, M.; Zannoni, C. *Chem. Phys. Lett.* **2001**, *336*, 253.

(21) Berardi, R.; Muccioli, L.; Orlandi, S.; Ricci M.; Zannoni, C. *Chem. Phys. Lett.* **2004**, *389*, 373.

(22) Ego, C.; Marsitzky, D.; Becker, S.; Zhang, J. Y.; Grimsdale, A. C.; Müllen, K.; MacKenzie, J. D.; Silva, C.; Friend, R. H. *J. Am. Chem. Soc.* **2003**, *125*, 437.

(23) Becker, K.; Lupton, J. M. *J. Am. Chem. Soc.* **2006**, *128*, 6468.

(24) Fron, E.; Bell, T. D. M.; Vooren, A. V.; Schweitzer, G.; Cornil, J.; Beljonne, D.; Toele, P.; Jacob, J.; Müllen, K.; Hofkens, J.; der Auweraer, M. V.; Schryver, F. C. D. *J. Am. Chem. Soc.* **2007**, *129*, 610.

(25) Winokur, M. J.; Slinker, J.; Huber, D. L. *Phys. Rev. B* **2003**, *67*, 184106.

(26) Kawana, S.; Durrel, M.; Lu, J.; Macdonald, J. E.; Grell, M.; Bradley, D. D. C.; Jukes, P. C.; Jones, R. A. L.; Bennett, S. L. *Polymer* **2002**, *43*, 1907.

(27) Somma, E.; Chi, C.; Loppinet, B.; Grinshtein, J.; Graf, R.; Fytas, G.; Spiess, H. W.; Wegner, G. *J. Chem. Phys.* **2006**, *124*, 204910.

(28) Güntner, R.; Farrell, T.; Scherf, U.; Miteva, T.; Yasuda, A.; Nelles, G. *J. Mater. Chem.* **2004**, *14*, 2622.

(29) Surin, M.; Hennebicq, E.; Ego, C.; Marsitzky, D.; Grimsdale, A. C.; Müllen, K.; Brédas, J. L.; Lazzaroni, R.; Leclere, P. *Chem. Mater.* **2004**, *16*, 994.

(30) Johnston, S. J.; Low, R. J.; Neal, M. P. *Phys. Rev. E* **2002**, *65*, 051706.

(31) Orlandi, S.; Berardi, R.; Steltzer, J.; Zannoni, C. *J. Chem. Phys.* **2006**, *124*, 124907.

(32) Berardi, R.; Fava, C.; Zannoni, C. *Chem. Phys. Lett.* **1998**, *297*, 8.

(33) Dewar, M. J. S.; Zoebisch, E. G.; Healy, E. F.; Stewart, J. J. P. *J. Am. Chem. Soc.* **1985**, *107*, 3902.

(34) Cornell, W. D.; Cieplak, P.; Bayly, C. I.; Gould, I. R.; Merz Jr., K. M.; Ferguson, D. M.; Spellmeyer, D. C.; Fox, T.; Caldwell, J. W.; Kollman, P. A. *J. Am. Chem. Soc.* **1995**, *117*, 5179.

(35) Jäckel, F.; Feyter, S. D.; Hofkens, J.; Köhn, F.; Schryver, F. C. D.; Ego, C.; Grimsdale, A. C.; Müllen, K. *Chem. Phys. Lett.* **2002**, *362*, 534.

(36) Frenkel, D.; Smit, B.; Academic Press: San Diego, 1996.

(37) Ridley, J.; Zerner, M. C. *Theor. Chim. Acta* **1973**, *32*, 111.

(38) In *Charge and Energy Transfer Dynamics in Molecular Systems*; May, V., Kühn, O., Eds.; Wiley: Berlin, 2000.

(39) AMPAC (Semiempirical Quantum Mechanics), Version 6.0. Semichem, Shawnee, KS, **1997**.

(40) Hennebicq, E.; Deleener, C.; Brédas, J. L.; Scholes, G. D.; Beljonne, D. *J. Chem. Phys.* **2006**, *125*, 054901.

(41) Cornil, J.; Gueli, I.; Dkhissi, A.; Sancho-Garcia, J. C.; Hennebicq, E.; Calbert, J. P.; Lemaur, V.; Beljonne, D.; Brédas, J. L. *J. Chem. Phys.* **2003**, *128*, 6615.

(42) Engström, S.; Lindberg, M.; Johansson, L. E.-A. *J. Chem. Phys.* **1988**, *89*, 204.

(43) Rose, M. E. *Elementary Theory of Angular Momentum;* Wiley: New York, 1957.

(44) Anderson, E.; Bai, Z.; Bischof, C.; Demmel, J.; Dongarra, J.; Croz, J. D.; Greenbaum, A.; Hammarling, S.; McKenney, A.; Ostrouchov, S.; Sorensen, D. *LAPACK Users' Guide;* SIAM, 1996.

TABLES

TABLE 1: Parameters used in the multisite Gay-Berne intermolecular potential.

fragment[a]	ϵ_x	ϵ_y	ϵ_z	σ_x	σ_y	σ_z	r_x	r_y	r_z	α	β	γ
	(kcal/mol)			(Å)			(Å)			(deg.)		
3F	7.0	7.0	1.0	13.0	13.0	30.0	0.0	0.0	0.0	0.0	0.0	0.0
PE1	26.0	2.0	1.0	4.0	10.0	16.5	0.4	1.0	17.3	0.0	15.0	30.0
PE2	26.0	2.0	1.0	4.0	10.0	16.5	1.5	1.2	-17.3	0.0	-15.0	-30.0
DMB1	0.7	4.5	0.7	9.0	5.0	10.0	2.3	1.0	23.9	0.0	15.0	20.0
DMB2	0.7	4.5	0.7	9.0	5.0	10.0	3.4	1.2	-23.9	0.0	-15.0	-20.0

[a]3F: terfluorene, PE1-2: end-capping perylenes, DMB1-2: dimethylbenzenes. A space-filling model of the molecule with the five fragments rendered as transparent ellipsoids is shown in Figure 1.

TABLE 2: Charge reduction schemes (CRS) tested in the energy transfer simulations and computation speed factors.

scheme	number of charges		speed factor
	terfluorene	perylene	
FULL	83	52	1×
CRS1	6	11	7.7×
CRS2	4	11	8.2×
CRS3	2	11	8.4×
ICRS3	2 (INTER), 83 (INTRA)	11 (INTER), 52 (INTRA)	8.4×
ICRS4	2 (INTER), 83 (INTRA)	4 (INTER), 52 (INTRA)	8.5×

FIGURE CAPTIONS

Figure 1. Structure of the perylene end-cappec terfluorene molecule and its CPK model embedded within five partially overlapping ellipsoids (transparent rendering) representing the Gay-Berne coarse-grained description. Ellipsoid positions and orientations are reported in Table 1. The size of the central ellipsoid takes into account the average volume of the octyl chains (replaced by methyls here; see text for details).

Figure 2. Snapshot of a glassy configuration of $N = 1000$ molecules at $T^* = 2$, $P^* = 5$. Molecules are color-coded according to their orientation, helping the identification of aligned domains.

Figure 3. Time dependence of the excitation probability, modeled with the full set of transition charges, of the initially excited terfluorene (a, also in the inset), the perylenes attached to it (b), all perylenes on other molecules (c) and all terfluorenes on other molecules (inset, d).

Figure 4. Charge distributions associated with the $g \rightarrow e$ transition, color coded according to the palette (units e/Å), obtained from the full set of charges for perylene (a) and terfluorene (b) and from a reduction scheme involving 11 charges on perylene (c) and 6 charges on terfluorene (d). Positions of the reduced charges in the molecular frame (e, f, negative charges: black, positive charges: cyan).

Figure 5. Energy transfer (ET) rate map, calculated with all atomic transition charges (a) or with the tested charge reduction schemes (see Table 2) CRS1, CRS2 and CRS3 (b, c and d, respectively), from a terfluorene (donor), fixed at the origin, to a perylene (acceptor) placed at the sites of a grid from −20 to 20 Å at 1 Å resolution, on the xy plane (points corresponding to intermolecular separations of unrealistically high interaction energy have been removed, see text for details). The map in (a) is color-coded according to the value of the donor–acceptor energy transfer rate (ps^{-1}) whereas the other maps are color-coded according to the percent deviation from (a) of the three CRS.

Figure 6. Time dependence of the excitation probability. Comparison between the full charge model (thick line, same a, b and c plots of Figure 3) and the three charge reduction schemes (CRS) chosen (see text for details). Inset I: detail of the intramolecular energy transfer peak (perylenes attached to the initially excited terfluorene) showing that, at shorter times, the deviations of the CRS from the full charge calculation are larger than the statistical uncertainties. Inset II: detail of the intermolecular energy transfer relaxation (all perylenes on other molecules) showing that, at longer times, the deviations of the CRS from the full charge calculation are within the statistical uncertainties.

Figure 7. Time dependence of the excitation probability. Comparison between the full charge model (thick line, same a, b and c plots of Figure 3) and two "improved" charge reduction schemes (ICRS3 and ICRS4, see Table 2) where the intramolecular transfers are modeled using the full set of transition charges. Inset I and II are a magnification of a small area (smaller than in Figure 6) showing that the results obtained with these schemes are nearly identical to the full charge model.

Figure 8. Application of the charge reduction scheme ICRS3 (see Table 2) to compare the case of a diffusion process limited by the intramolecular transfer rate from terfluorene to perylene ("INTRA < INTER") to the previous case ("INTRA > INTER"). a′, b′ and c′ dashed lines are to be compared with solid lines a, b and c (same plots of Figure 3), respectively. The corresponding energy transfers involved are also depicted in the inset.

FIGURES

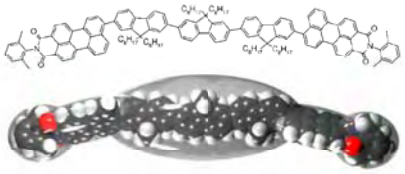

Figure 1.

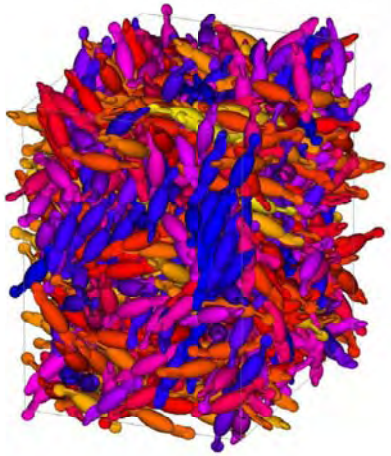

Figure 2.

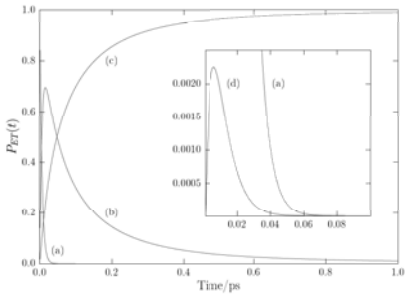

Figure 3.

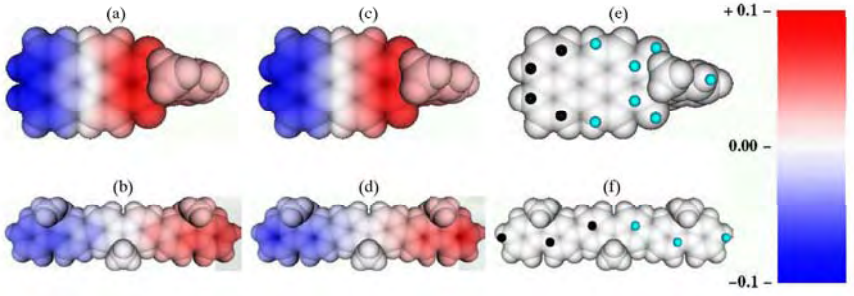

Figure 4.

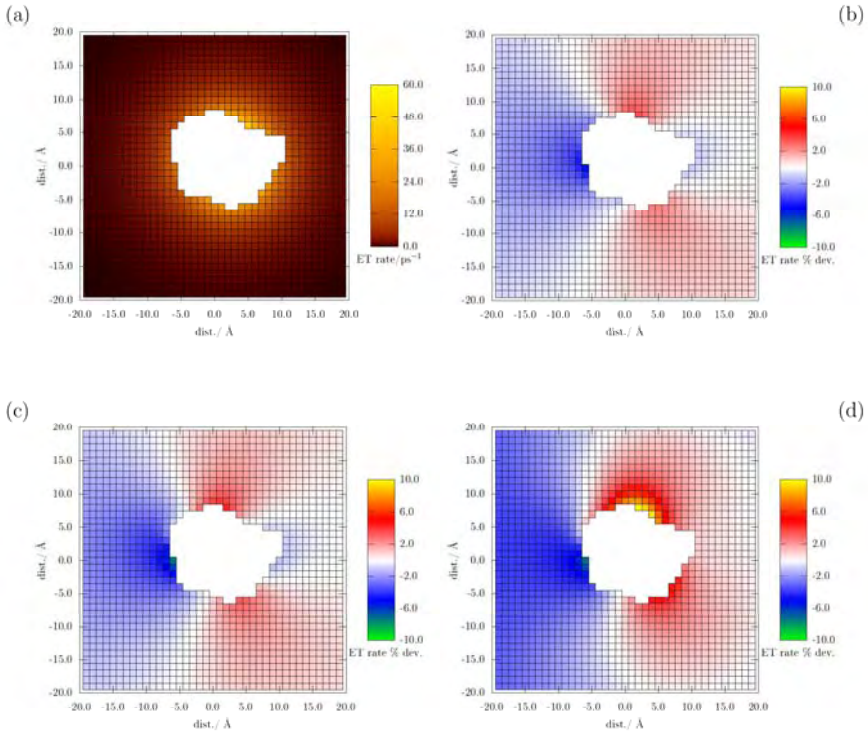

Figure 5.

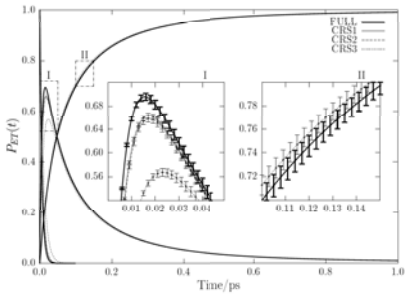

Figure 6.

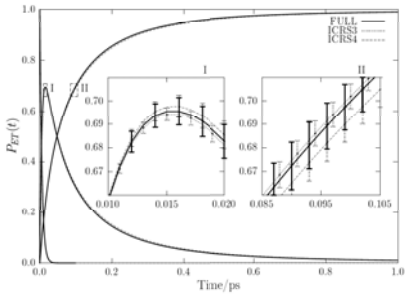

Figure 7.

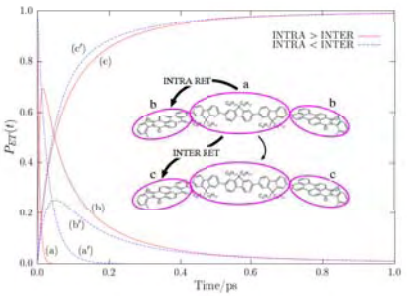

Figure 8.